nature geoscience

SUPPLEMENTARY INFORMATION

DOI: 10.1038/NGEO989

Supplementary Material for 'Photolysis of sulphuric acid as the source of sulphur oxides in the mesosphere of Venus'

Xi Zhang[1*], Mao-Chang Liang[2,3,4], Franck Montmessin[5,6], Jean-Loup Bertaux[5,6], Christopher Parkinson[7], Yuk L. Yung[1]

[1] *Division of Geological and Planetary Sciences, California Institute of Technology, Pasadena, CA, 91125, USA*

[2] *Research Center for Environmental Changes, Academia Sinica, Taipei, Taiwan*

[3] *Graduate Institute of Astronomy, National Central University, Zhongli, Taiwan*

[4] *Institute of Astronomy and Astrophysics, Academia Sinica, Taipei, Taiwan*

[5] *LATMOS, CNRS/INSU/IPSL, Université de Versailles-Saint-Quentin, Quartier des Garennes, 78280 Guyancourt, France*

[6] *Universite´ Pierre et Marie Curie, 75252, Paris, France*

[7] *Department of Atmospheric, Oceanic, and Space Sciences, University of Michigan, 2455 Hayward Street, Ann Arbor, MI 48109, USA*

*contact email: xiz@gps.caltech.edu

DOI: 10.1038/NGEO989

In this supplementary material, we will first provide the details of the SPICAV solar occultation measurements of sulphur dioxide at the terminator in section 1. In section 2 we will show how we obtain the H_2SO_4 saturation vapor pressure (SVP) for this study, and discuss the uncertainties of our calculation and the other possible factors that might influence the H_2SO_4 SVP in the Venus mesosphere. The Caltech/JPL kinetics photochemical model is described in section 3. The model parameters and the chemical reaction rates of other sulphur oxides (SO and SO_3) are also presented.

1. SPICAV measurements

Solar occultation is known to be one of the most reliable and accurate techniques to probe planetary atmospheres. It requires no instrument calibration and is only based on the simplest laws of radiative transfer. Spectroscopy for Investigation of Characteristics of the Atmosphere of Venus (SPICAV) onboard Venus Express (see previous publications[1-2] for more description) has provided a wealth of high-quality data through this technique during several orbits since 2006. The solar occultation performed by SPICAV probes the state of the atmosphere at the terminator, which is known to possess a very peculiar dynamical regime with downwelling and upwelling motions streamlining close together, potentially creating strong spatial contrasts at small scales that are unattainable by the sub-mm JCMT beam from the ground-based measurement. This could be one of the possible reasons that cause the incompatible SO_2 abundances from the two observation techniques[3]. However, both of the ground-based sub-mm spectroscopy[3] and the Venus Express occultation measurements[4] suggest the presence of an unexpected separate SO_2 layer above 90 km in the Venus mesosphere.

The observed SO_2 profile used in Fig. 1a is taken in orbit 334, at longitude 315.7°, latitude -10.2° and the local time 18h. Errors on SO_2 concentrations are established during spectral inversion as a by-product of the Levenberg-Marquardt routine used for the chi-square minimization (square root of the diagonal terms in the covariance matrix). They are then propagated after vertical inversion following. Error bar determination emplys the same procedure as the one used to derive O_3, CO_2 and aerosol profils on Mars with SPICAM[5-7].

2. H_2SO_4 saturation vapor pressure (SVP)

The SVP of sulphuric acid is determined by the relative humidity of H_2SO_4-H_2O solution and the atmospheric temperature. The weight percent of sulphuric acid is assumed to be 85% for the upper clouds[8] and 75% for the upper haze layer[9] at about 70-90 km. Recent solar occultation measurements by SPICAV/SOIR onboard Venus Express[10] suggest a bimodal distribution of particle sizes if one assumes that the haze droplets are composed of 75% H_2SO_4, and the same measurements suggest that only very small size particles (less than 0.2 micron) exist above 90 km. Since there are more collisions of aerosol particles with H_2O molecules than with H_2SO_4 molecules, the sulfate aerosol will quickly establish equilibrium with respect to water. The relative humidity of H_2O in the mesosphere decreases with height above the cloud top because the temperature is increasing and the mixing ratio of water vapor is decreasing with altitude[11]. Therefore, the weight percent of the droplets could be larger than 75%, which results in higher H_2SO_4 vapor pressure. The more highly concentrated H_2SO_4 has a higher extinction coefficient due to the Lorentz relation[12], leading to even smaller retrieved particle size. Therefore, the Kelvin effect[13], by which vapor pressure increases over a curved interface,

DOI: 10.1038/NGEO989

would become more important and enhance the gaseous H_2SO_4 abundance in the mesosphere.

Stull's measurements[14] of the SVP of H_2SO_4 can be fitted by the expression $\log_{10}P(H_2SO_4) = -3954.90/T + 9.4570$, for a temperature range approximately between 420 K and 580 K, where $P(H_2SO_4)$ is the SVP of H_2SO_4 in mmHg and T is temperature. Fig. S1 shows this in comparisons with the expression from Richardson et al.[15] given by $\log P(H_2SO_4) = (20.70 \pm 1.74) - (9360 + 499)/T$ and the expression from Ayers et al.[16] corrected by Kulmala and Laaksonen[17]. We see from this difference in the three SVP expressions that we can obtain significantly difference SVP values for temperature values of interest to the mesosphere of Venus (grey area in Fig. S2). Over the temperature range of our model atmosphere, our calculation shows that the SVP from Stull is larger than that from Ayers et al. by a factor of ~1000 and ~20, and larger than that from Richardson et al. by a factor of ~12 and ~7, corresponding to 179 K (0.0036 K^{-1}) at the bottom of our model atmosphere and 274 K (0.0056 K^{-1}) at the top. Thus, the expression from Stull allows for the SVP of H_2SO_4 to be large enough to produce higher concentrations of SO_2 at ~100 km. If even higher values for the SVP were used as in our sensitivity study, higher abundances of H_2SO_4 at 100km would be obtained, resulting in even higher concentrations of SO_2 as observed by Belyaev et al.[4]. The expression from Stull has been used by Wong et al.[18] and Parkinson et al.[19]. The actual H_2SO_4 vapor mixing ratio is dependent on a number of factors, including water abundance, sulphuric acid concentration, degree of supersaturation, and the range of validity of the SVP extrapolation[18].

3. Photochemical model

The Caltech/JPL kinetics photochemical model solves the continuity equation for all important species in the Venus atmosphere above the cloud top and includes the oxygen, chlorine and sulphur chemistry recommended by Yung et al.[20] and Mills[21] with updated reaction coefficients. The model covers the Venus atmosphere from 58 km (cloud top) to 112 km. Table S1 lists the important reactions involving SO, SO_2 and SO_3.

Venus is a slowly rotating planet with very high temperature contrast between its day side and night side. The unexpected warm layer on the night side at about 90 km was detected by SPICAV and is believed to be the result of adiabatic heating by downwelling motion on the night side[11]. The aerosol particles would evaporate when transported by winds to the night side. In this study, we adopt the temperature profile measured in orbit 104 at latitude 4° S and local time 23:20 h (black curve in the Fig. 1 of Bertaux et al.[11]). This temperature profile has a peak value about 234K around 97km which is larger than the other measurements[22-25] by 40-50 K. Fig. S2a shows the daytime and nighttime temperature profiles.

Fig. S2b shows the H_2SO_4 saturated vapor mixing ratio profiles given by Stull[14]. In this study, the H_2SO_4 vapor pressure is calculated based on H_2SO_4 weight percent as 85% below 70 km, 75% from 70 to 90 km and 100% (i.e., pure sulphuric acid) above 90 km. We applied a scaling factor to the saturation ratio on the night time H_2SO_4 SVP profile above 90 km for the sensitivity study. The observed SO_2 mixing ratio at ~69 km by Solar Occultation in the Infrared (SOIR) instrument onboard Venus Express is larger than 0.1 ppm and agrees with the natural variability of SO_2 with time above the cloud top, which is a well-known problem[26]. It may indicate either there is more SO_2 within the clouds or the eddy mixing processes above the cloud top transport the SO_2 more efficiently. In this study, SO_2 mixing ratio at the lower boundary is set at 100 ppm to reproduce the data.

DOI: 10.1038/NGEO989

However, this adjustment has no effect on the SO_2 abundances above 90 km. The eddy mixing coefficient profile from Mills[21] is shown in Fig. S2c.

Figures S3 and S4 show the main production/loss rate profiles of SO and SO_3 as function of altitude, respectively. The upper panels (a and b) and lower panels (c and d) in each figure refer to models B and C, respectively. Each curve corresponds to a reaction in Table S1. The main sources of SO are the SO_3 photolysis and the oxidization of sulphur atoms, and the main loss is through photolysis to yield sulphur atoms in the upper atmosphere. SO is also oxidized back to SO_2 by the reactions with O, ClCO and $ClCO_3$. Without H_2SO_4 photolysis, SO_3 is only produced by SO_2 reacting with O and $ClCO_3$, the reaction rates of which decrease rapidly with altitude. Therefore, only photodissociation of sulphuric acid is able to provide the SO_3 source in the mesosphere of Venus. SO_3 is mostly destroyed by the photolysis and reacting with water to form H_2SO_4 and also can be reduced to SO_2 by reacting with SO and O atoms. The important reaction pathways of sulphur chemistry are summarized in Fig. 2 of the main text.

Figure Legends

Figure S1 | H_2SO_4 saturation vapor pressure as function of temperature. Three SVPs are calculated by Stull[14] (red), by Richardson et al.[15] (green), and by Ayers et al.[16] corrected by Kulmala and Laaksonen[17] (blue). The filled diamonds indicate the ranges of the experimental data. The gray area shows the temperature range of the Venus mesosphere.

Figure S2 | Model paramenters. a, daytime (black) and nighttime (red) temperature profiles as function of altitude. **b**, H_2SO_4 saturated vapor pressure profiles corresponding to the temperature profiles on the left. **c**, eddy diffusion coefficient profile from Mills[21].

Figure S3 | Rates of important reactions involved in producing (a and c) and destroying (b and d) SO for models B (a and b) and C (c and d). Different colors refer to different reactions listed in Supplementary Table S1. For panels **a** and **c**, R3 (blue), R7 (red). For **b** and **d**, R1 (purple), R6 (blue), R9 (green), R10 (light green), R11 (black), R15 (red).

Figure S4 | Rates of important reactions involved in producing (a and c) and destroying (b and d) SO_3 for models B (a and b) and C (c and d). Different colors refer to different reactions listed in Supplementary Table S1. For **a** and **c**, R5 (black), R12 (red), R13 (blue). For **b** and **d**, R4 (black), R8 (red), R14 (blue), R15 (green).

DOI: 10.1038/NGEO989

Table S1

[a] Important Reactions Involving SO, SO_2 and SO_3

Reaction	Rate Constant[b]	Reference
(R1) $SO \rightarrow S + O$	3.61×10^{-4}	c
(R2) $SO_2 \rightarrow S + O_2$	1.38×10^{-6}	c
(R3) $SO_2 \rightarrow SO + O$	1.92×10^{-4}	c
(R4) $SO_3 \rightarrow SO_2 + O$	3.94×10^{-5}	27
(R5) $H_2SO_4 \rightarrow SO_3 + H_2O$	2.72×10^{-7}	28
(R6) $ClO + SO \rightarrow Cl + SO_2$	2.80×10^{-11}	29
(R7) $S + O_2 \rightarrow SO + O$	2.30×10^{-12}	29
(R8) $SO_3 + H_2O \rightarrow H_2SO_4$	$2.26\times10^{-43} T\, e^{-(6544/T)}[H_2O]$	30
(R9) $O + SO + M \rightarrow SO_2 + M$	$k_0 = 4.50\times10^{-27} T^{1.6}$	31-32
(R10) $ClCO_3 + SO \rightarrow Cl + SO_2 + CO_2$	1.00×10^{-11}	c
(R11) $SO + SO + M \rightarrow (SO)_2 + M$	$k_0 = 4.40\times10^{-31}$	c
	$k_\infty = 1.00\times10^{-11}$	
(R12) $O + SO_2 + M \rightarrow SO_3 + M$	$k_0 = 4.00\times10^{-32} e^{-(-1000/T)}$	33
(R13) $ClCO_3 + SO_2 \rightarrow Cl + SO_3 + CO_2$	1.00×10^{-15}	c
(R14) $O + SO_3 \rightarrow SO_2 + O_2$	$2.32\times10^{-16} e^{-(-487/T)}$	34
(R15) $SO + SO_3 \rightarrow 2SO_2$	2.00×10^{-15}	35

[a] The model includes all reactions from Mills (1998)[21].

[b] M represents the third body such as CO_2 for three-body reactions. Two-body rate constants and high-pressure limiting rate constants for three-body reactions (k_∞) are in units of cm^3s^{-1}. Low-pressure limiting rate constants for three-body reactions (k_0) are in units of cm^6s^{-1}. Photolysis coefficients (J values) refer to the top of mesosphere (112 km in the model).

[c] See discussion in Mills (1998)[21] and references therein.

References

1 Bertaux, J. L. SPICAV on Venus Express: three spectrometers to study the global structure and composition of the Venus atmosphere. *Planet. Space Sci.* **55**, 1673-1700 (2007).

2 Titov, D. V. Venus Express: Scientific goals, instrumentation, and scenario of the mission. *Cosmic Res.* **44**, 334-348 (2006).

3 Sandor, B. J., Clancy, R. T., Moriarty-Schieven, G. & Mills, F. P. Sulfur chemistry in the Venus mesosphere from SO_2 and SO microwave spectra. *Icarus* **208**, 49-60 (2010).

4 Belyaev, D. *et al.* Vertical Profiling of SO_2 above Venus' Clouds by means of SPICAV/SOIR Occultations. *Bull. Am. Astron. Soc.* **41**, 1120-1120 (2009).

5 Lebonnois, S. *et al.* Vertical distribution of ozone on Mars as measured by SPICAM/Mars Express using stellar occultations. *J. Geophys. Res.* **111**, E09S05 (2006).

6 Montmessin, F. Stellar occultations at UV wavelengths by the SPICAM instrument: Retrieval and analysis of Martian haze profiles. *J. Geophys. Res.* **111**, E09S09 (2006).

7 Quémerais, E. *et al.* Stellar occultations observed by SPICAM on Mars Express. *J. Geophys. Res.* **111**, E09S04 (2006).

8 Krasnopolsky, V. A. & Pollack, J. B. H_2O-H_2SO_4 system in Venus' clouds and OCS, CO, and H_2SO_4 profiles in Venus' troposphere. *Icarus* **109**, 58-78 (1994).

9 Kawabata, K. Cloud and haze properties from Pioneer Venus polarimetry. *J. Geophys. Res.* **85**, 8129-8140 (1980).

10 Wilquet, V. *et al.* Preliminary characterization of the upper haze by SPICAV/SOIR solar occultation in UV to mid-IR onboard Venus Express. *J. Geophys. Res.* **114**, E00B42 (2009).

11 Bertaux, J. L. *et al.* A warm layer in Venus' cryosphere and high-altitude measurements of HF, HCl, H_2O and HDO. *Nature* **450**, 646-649 (2007).

12 Goody, R. M. & Yung, Y. L. *Atmospheric Radiation: Theoretical Basis*. 299-299 (Oxford Univ. Pr., Oxford, 1995).

13 Seinfeld, J. H. & Pandis, S. N. *Atmospheric Chemistry and Physics: From Air Pollution to Climate Change*. 463-463 (John Wiley & Sons, Inc., New York, 2006).

14 Stull, D. R. Vapor pressure of pure substances—Inorganic compounds *Ind. Eng. Chem.* **39**, 540-550 (1947).

15 Richardson, C. B., Hightower, R. L. & Pigg, A. L. Optical measurement of the evaporation of sulfuric acid droplets. *Appl. opt.* **25**, 1226-1229 (1986).

DOI: 10.1038/NGEO989

16 Ayers, G. P., Gillett, R. W. & J. L. Gras. On the vapor pressure of sulfuric acid. *Geophys. Res. Lett.* **7**, 433-436 (1980).

17 Kulmala, M. & Laaksonen, A. Binary nucleation of water-sulphuric acid system: Comparison of classical theories with different H_2SO_4 saturation vapour pressures. *J. Chem. Phys.* **93**, 696-701 (1990).

18 Wong, A. S., Atreya, S. K. & Encrenaz, T. Chemical markers of possible hot spots on Mars. *J. Geophys. Res.* **108**, E4, 5026 (2003).

19 Parkinson, C. D., Atreya, S. K., Mills, F., Yung, Y. L. & Wong, A.-S. Photochemical Distributon of Venusian Sulfur and Halogen Species. *Bull. Am. Astron. Soc.* **40**, 467-467 (2008).

20 Yung, Y. L. & DeMore, W. B. Photochemistry of the Stratosphere of Venus: Implications for Atmospheric Evolution. *Icarus* **51**, 199-247 (1982).

21 Mills, F. P. I. Observations and Photochemical Modeling of the Venus Middle Atmosphere. II. Thermal Infrared Spectroscopy of Europa and Callisto. *PhD thesis, California Institute of Technology* 1-277 (1998).

22 Clancy, R. T. Observational definition of the Venus mesopause: vertical structure, diurnal variation, and temporal instability. *Icarus* **161**, 1-16 (2003).

23 Lellouch, E. Global circulation, thermal structure, and carbon monoxide distribution in Venus' mesosphere in 1991. *Icarus* **110**, 315-339 (1994).

24 Ohtsuki, S. Distributions of the Venus 1.27-μm O_2 airglow and rotational temperature. *Planet. Space Sci.* **56**, 1391-1398 (2008).

25 Zasova, L. V. Structure of the Venusian atmosphere from surface up to 100 km. *Cosmic Res.* **44**, 364-383 (2006).

26 Belyaev, D. *et al.* First observations of SO_2 above Venus' clouds by means of Solar Occultation in the Infrared. *J. Geophys. Res.* **113**, E00B25 (2008).

27 Burkholder, J. B. & McKeen, S. UV absorption cross sections for SO_3. *Geophys. Res. Lett.* **24**, 3201-3204 (1997).

28 Mills, M. J. *et al.* Photolysis of sulfuric acid vapor by visible light as a source of the polar stratospheric CN layer. *J. Geophys. Res.* **110**, D08201 (2005).

29 Sander, S. P. *et al. Chemical kinetics and photochemical data for use in atmospheric studies : evaluation number 15*. (Jet Propulsion Laboratory, California Institute of Technology, Pasadena, CA, 2006).

30 Lovejoy, E. R., Hanson, D. R. & Huey, L. G. Kinetics and products of the gas-phase reaction of SO_3 with water. *J. Phys. Chem.* **100**, 19911-19916 (1996).

31 Grillo, A. Infrared measurements of sulfur dioxide thermal decomposition rate in shock waves. *J. chem. phys.* **70**, 1634-1636 (1979).

32 Singleton, D. L. & Cvetanovi´c, R. J. Evaluated chemical kinetic data for the reactions of atomic oxygen $O(^3P)$ with sulfur containing compounds. *J. Phys. Chem. Ref. Data* **17**, 1377-1437 (1988).

33 Atkinson, R. Evaluated kinetic and photochemical data for atmospheric chemistry: Volume I-gas phase reactions of O_x, HO_x, NO_x and SO_x species. *Atmos. chem.phys.* **4**, 1461-1738 (2004).

34 Jacob, A. & Winkler, C. A. Kinetics of the reactions of oxygen atoms and nitrogen atoms with sulfur trioxide. *J. Chem. Soc. Faraday Trans. 1* **68**, 2077-2082 (1972).

35 Chung, K., Calvert, J. G. & Bottenheim, J. W. The photochemistry of sulfur dioxide excited within its first allowed band (3130 Å) and the forbidden band (3700-4000 Å). *Int. J. Chem. Kinetics* **7**, 161-182 (1975).

DOI: 10.1038/NGEO989

Figure S1

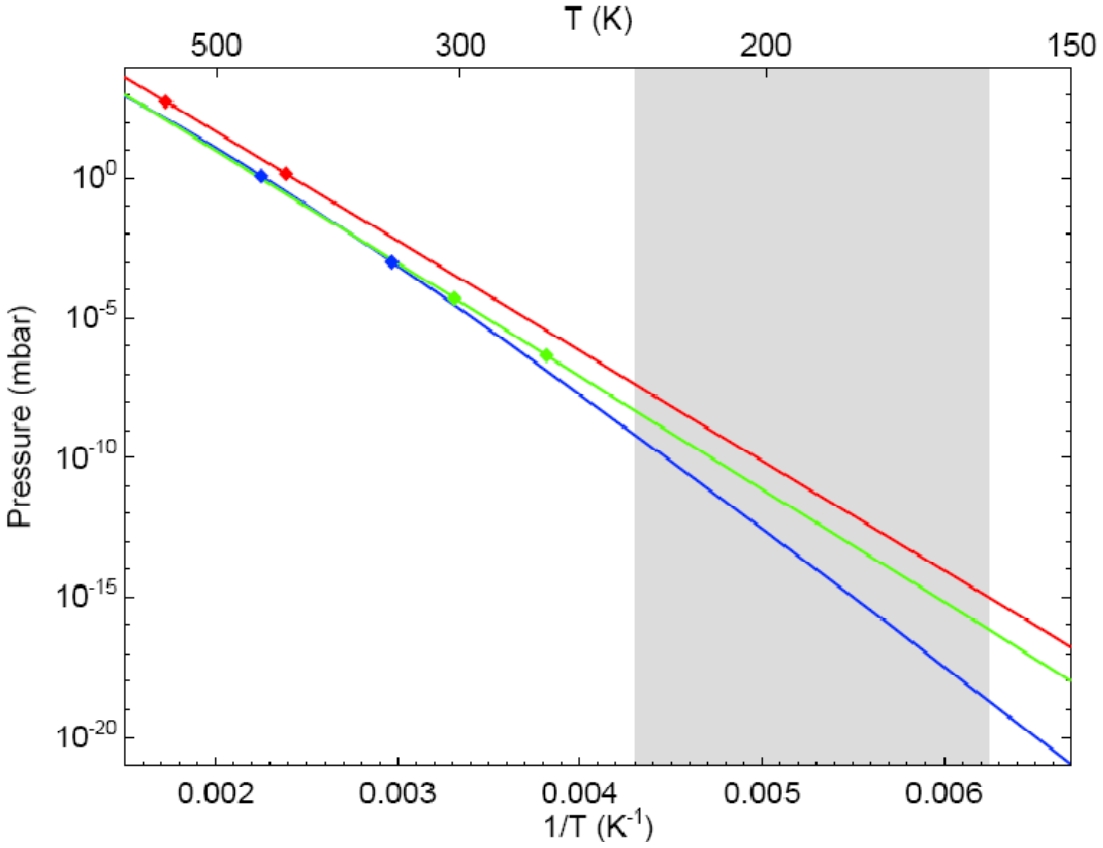

Figure S2

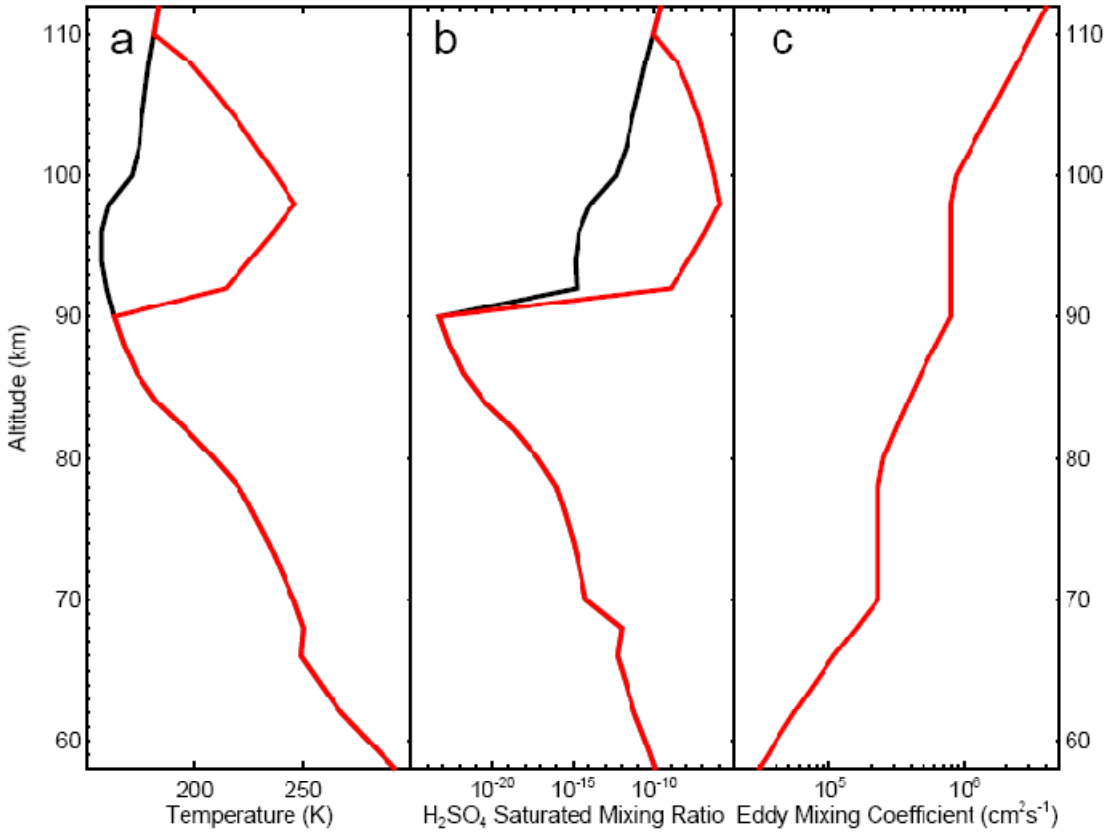
a
b
c
110
100
90
80
70
60
Altitude (km)
200
250
Temperature (K)
10^{-20}
10^{-15}
10^{-10}
H_2SO_4 Saturated Mixing Ratio
10^{5}
10^{6}
Eddy Mixing Coefficient (cm^2s^{-1})

DOI: 10.1038/NGEO989

Figure S3

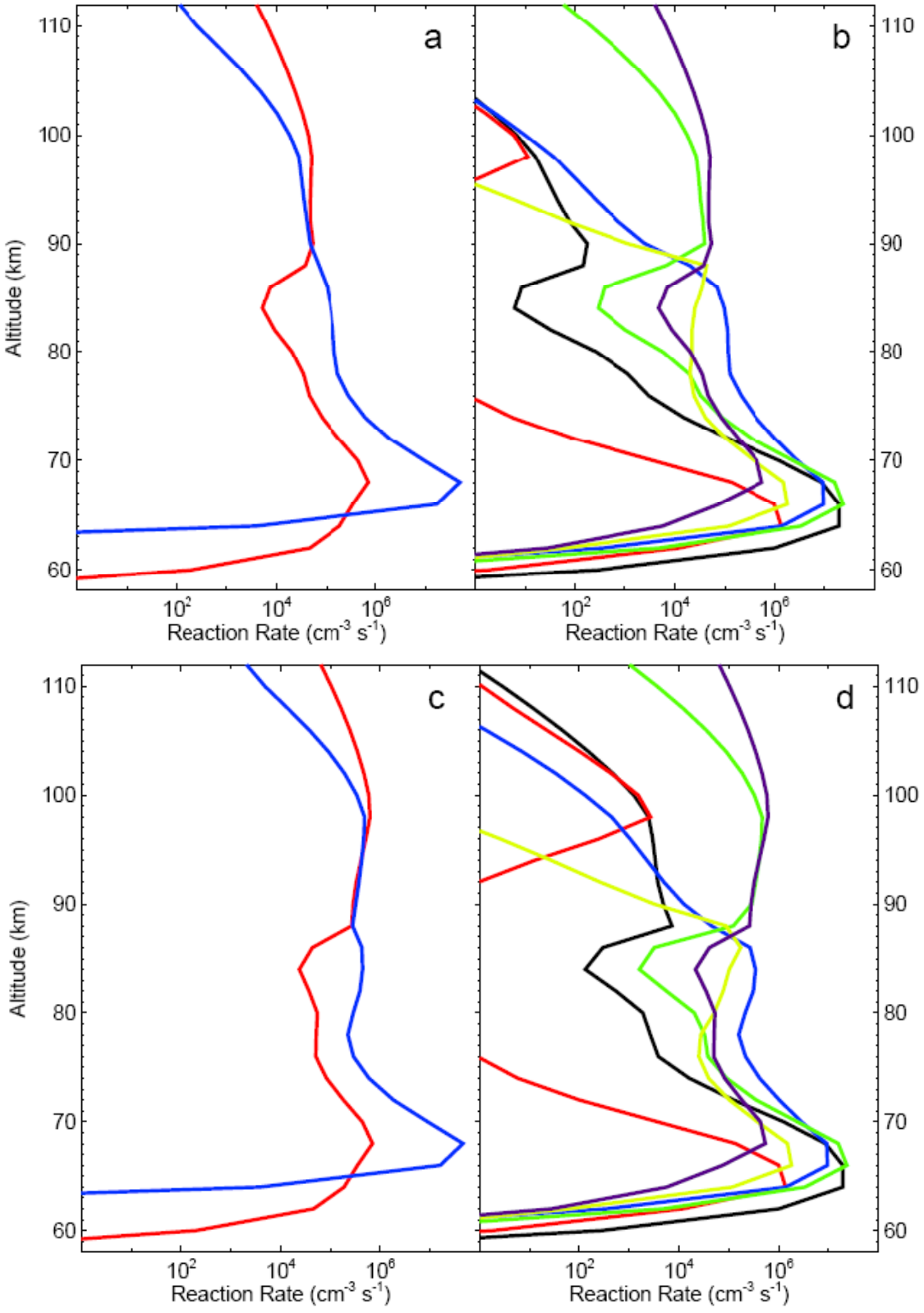

Figure S4

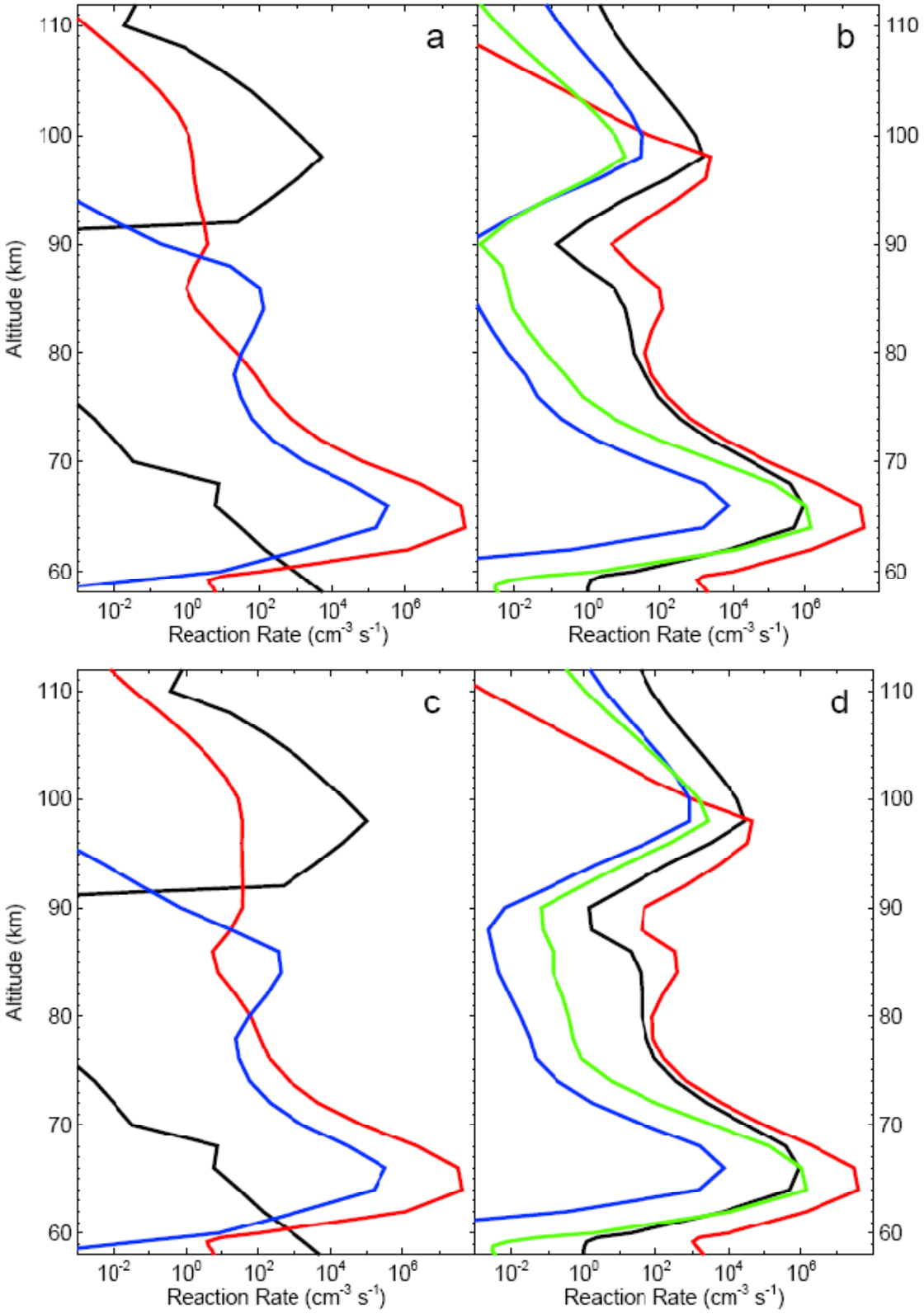
a
b
c
d
Altitude (km)
Reaction Rate (cm^{-3} s^{-1})
110
100
90
80
70
60
10^{-2}
10^{0}
10^{2}
10^{4}
10^{6}